Optimal Sizing and Analysis of Hybrid Battery Packs for Electric Racing Cars

Stefano Radrizzani, *Graduate Student Member, IEEE*, Giorgio Riva, Giulio Panzani, *Member, IEEE*, Matteo Corno, Sergio M. Savaresi, *Senior Member, IEEE*

***Abstract*—The electrification trend is spreading not only in the field of traditional vehicles, but also in the racing one, with challenging power and range demands. As an example, the next generation of Formula E will increase power up to 600 kW, almost triplicating the actual standards. In this paper, we investigate the potential benefits of hybrid battery packs in a racing scenario. Hybrid battery packs combine different cell technologies aiming at exploiting their respective high-power and high-energy densities. To this purpose, we formulate a co-design optimization problem that finds the optimal hybrid battery pack configuration to minimize the race time, on a given circuit. As a case study, the next generation of Formula E on the 2021 Rome Formula E ePrix is considered. Results show a significant gain in terms of race time, compared to a single cell chemistry battery pack. Moreover, the analysis points out interesting results on the optimal power split strategy and the role of mechanical brakes.**

***Index Terms*—Electric Racing Cars, Battery Sizing, Optimization, Optimal Control, Co-Design**

I. Introduction

BESIDE their appeal for sports passionate, vehicle competitions have always been a challenging environment that led to important technological and scientific progress, in particular when dealing with vehicle dynamics. Among the several areas – such as aerodynamics, tires, mechanical component design and materials – the powertrain witnessed several important changes in the latest years, following one of the most important trends for the mass-market automotive: vehicle electrification. Indeed, Formula 1 is currently living its hybrid era and the full-electric Formula E championship is gaining more popularity.

This powertrain evolution pushed several advancements in the vehicle dynamics control, in particular with the development of energy management strategies (EMS). In fact, to fully exploit the benefits of hybrid powertrains, a proper management of the internal combustion engine and the battery power is required; similarly in full-electric vehicles it is mandatory to balance the amount of regenerative and mechanical braking, according to the battery state of charge and the brake intensity. In order to address these issues, *minimum lap/race time* approaches have been proposed: framed as constrained optimal control problems, they aim at computing throttle and brake commands, and possibly also steer, to minimize the vehicle lap/race time. They have been successfully employed in the development of optimal energy management strategies in different racing contexts: hybrid powertrain architectures [1], [2] but also full-electric competitions, like Roborace [3] or endurance [4]. Compared to the typical scenarios where hybrid or electric vehicles optimal EMS are discussed, the minimum lap time EMS differs in the definition and the role of the vehicle mission profile, also called driving-cycle. Usually, the driving-cycle is given *a-priori* and reflects the typical/expected vehicle usage; within the optimal control problem it plays the role of a constraint that must be satisfied. Opposite, when addressing a racing scenario, the mission profile directly impacts the ultimate goal of the design, i.e., the minimization of the lap/race time; as such, it is not known in advance and cannot be a-priori fixed and it is an outcome of the optimization process along with the desired EMS.

The performance of electrified powertrains, being hybrid or full-electric, is intimately bonded not only to the designed EMS but also to the architecture and size of their elements. Indeed, many works have shown that an optimization-based *co-design* (Co-OP) of the powertrain components along with their energy management yields further improvements with respect to the sole EMS design. References [5]–[7] apply such concept to hybrid powertrain in standard scenarios, whereas [8], [9] address a racing context, making use of the minimum lap/race time co-design paradigm respectively for hybrid and full-electric racing vehicles.

This work deals with *hybrid battery packs* (H-BPs), which is one of the emerging architectures for the next generation of full-electric powertrain. Hybrid battery packs are made of different cell technologies featuring complementary characteristics which cannot be simultaneously provided by a single cell type. In particular, H-BPs address the well-known trade-off between high-energy and high-power density by joining, in the same battery pack, different cells with complementary energy/power density properties [10].

The potential of H-BPs has been already discussed in literature. In the available works, the analysis focuses on the trade-off between an efficient usage of the battery energy, the battery size (in terms of either mass, volume or number of cells) [11]–[13] and the battery life [14]–[17]. To address these trade-offs, a monetary cost function that accounts for the energy and the battery components costs is frequently employed [11]–[13], [16] or, similarly, an affine combination of two competing cost functions is used [17]; alternatively, the multi-objective optimization results are analysed in terms of the resulting Pareto front [14], [15].

The authors are with Dipartimento di Elettronica, Informazione e Bioingegneria, Politecnico di Milano, Via G. Ponzio 34/5, 20133, Milan, Italy. {stefano.radrizzani, giorgio.riva, giulio.panzani, matteo.corno, sergio.savaresi}@polimi.it Corresponding author: Stefano Radrizzani. This paper has never been submitted elsewhere, previously.

In the present work, we aim at analyzing the advantages of H-BPs from a genuine vehicle dynamics perspective. To do so, we tackle the Formula E case study; specifically, the upcoming Generation 3 (Gen 3) vehicle that represents one of the most challenging racing scenario for electric powertrains. More in details, we compare the best simulated *2021 Rome Formula E ePrix* race time obtained with a single-cell BP powertrain against the one obtained using a hybrid-BP solution. For both powertrain architectures, an optimal co-design (Co-OP) approach is employed, based on the minimum race time paradigm, which is the most suitable and natural approach to address the proposed comparison. The two-layered Co-OP approach we recently presented in [9] is adopted for the design of the single-cell powertrain: it optimizes the choice of the cell technology and the BP size (external layer optimization) along with the EMS (internal layer optimization). For the hybrid battery pack, we here propose a three-layered extension. The external layer selects the best *high-energy* and *high-power* cell chemistry based on a model that correlates the fundamental cell properties, i.e., the energy density, the power density and the internal resistance. The intermediate optimization layer computes the size of each battery pack subsystem. Finally, the internal layer, properly reformulated for the hybrid-BP powertrain, computes the usage of the battery pack and dissipative mechanical braking during the entire race.

With respect to the available literature, this paper contributes in the following aspects.

Aim and scope. As mentioned, the objective of our research is to quantify the potentials of H-BPs from a vehicle dynamic perspective; in other words, how and if vehicle dynamics can be enhanced with a proper usage of H-BPs. This objective matches the needs of racing applications/context and has never been addressed before. Compared to the available literature, we employ a minimum lap/race time approach: such a choice reflects not only in the definition of a different and specific cost function, but also requires structural changes in the optimization problem settings, as it does not require any predefined mission profile to be solved.

Powertrain layout. In the present work, the availability of a mechanical braking torque is considered. This feature is seldom considered in the H-BP literature that typically assumes a complete regenerative braking. In our work, we specifically highlight the role of mechanical brakes, also comparing their usage with different H-BP configurations; the assessment of the duality between mechanical and regenerative braking is also an original outcome of the proposed analysis.

H-BP design. The proposed approach includes as H-BP design variables not only the configuration of the two high-energy and high-power battery packs but also their respective cell chemistry. On the contrary, in the available literature, the cell properties are typically predefined and fixed. To enable the inclusion of cell chemistries within the optimization variable set, we leverage a model, based on a deep literature analysis, that correlates the fundamental cell properties and well represent both the state-of-the-art and the trending cell technologies. Thus, in addition to providing indications regarding the benefits of H-BPs, the formulated Co-OP can be seen as a general tool; indeed, it can support the vehicle powertrain designer, not only in having a quantitative forecast of the battery layout, but also in orienting his/her choices in terms of cell types. Additionally, including the cell chemistries within the optimal design variables also provides an interesting assessment on how much the available (and shortly to come) cell technologies match the racing application needs.

The remainder of the paper is organized as follows: in Section II an overview on the commercialized and prototype Lithium-ion cell technology is given. In Section III, the optimization problem is formulated, and its numerical solution strategy is presented in Section IV. Finally, the numerical results for the Gen3 Formula E case study are discussed in Section V. The paper ends with some concluding remarks.

II. Lithium-Ion cell technologies Overview

The family of Lithium-ion (Li-ion) batteries is constituted by chemistries that use either different combinations of anode and cathode materials or different manufacturing processes. Currently, in the field of commercial electric or hybrid-electric vehicles, the most common cathode technologies employed are LMO (Lithium Manganese Oxide), LFP (Lithium Iron Phosphate), NCA (Lithium Nickel Cobalt Aluminum Oxide), NMC (Lithium Nickel Manganese Cobalt Oxide) [18], while the anode is typically composed of graphite (C). We refer to this set as **standard technologies**. NCA and NMC cover a wider slice of the market [19] than LMO and LFP. Indeed, the presence of cobalt in the cathode increases the energy density with respect to LFP, without generating a significant reduction of power density as for LMO. Nevertheless, LMO has the low cost as a principal advantage, therefore it is usually combined with NCM technology in order to temporarily increase its power density, providing high current boosts [18]. To visualize the performance of these standard technologies, in terms of energy and power density*, they are represented on the so-called Ragone plot, in Fig. 1. It is manifest how NMC and NCA are the most performing solutions, and this explains why they are be considered the standard technology in electrified vehicles. Indeed, as summarized in [18], NMC technology is the current most widespread technology on the market, used by Volkswagen, Honda, Renault and many others, while NCA is mainly used by Tesla.

The vehicle electrification trend has increased the number of studies aiming at exploring different possibilities to improve battery performance. In such a continuously evolving scenario, two research objectives can be identified: 1) the increase of energy density to either guarantee longer mileage or decrease vehicle weight, and 2) the increase of power density to allow faster charge/discharge rates.

Considering the former, different technologies are currently under development, among which, the most promising are: **(a) Lithium-metal anodes**: which improve energy density thanks to the lightness of the lithium (Li) [20], while still showing short cell lifespan and safety concerns; **(b) Silicon-based anodes**: which exploit the higher Silicon (Si) theoretical capacity than graphite and better cycling performance thanks

*In this work, energy and power density are defined at cell-level, considering the weight of the complete cell.

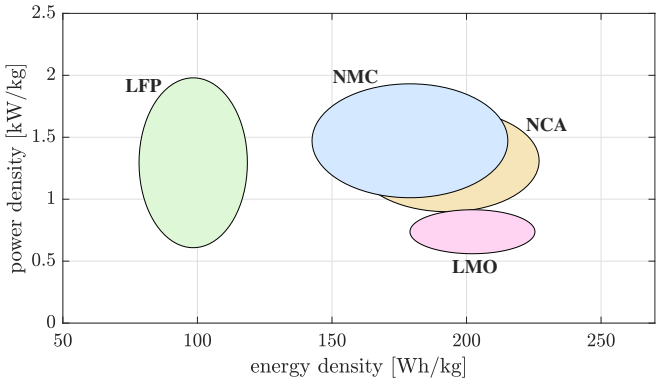

Fig. 1. Ragone Plot of current cell technologies.

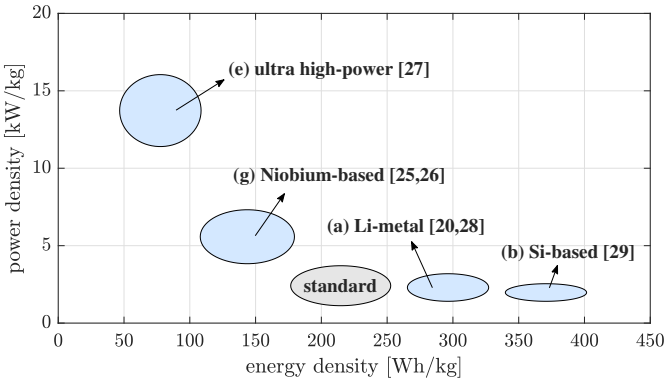

Fig. 2. Qualitative Ragone plot of the considered emerging cell technologies compared with the standard ones.

to nanowire strategies, meant to overcome the main drawbacks generated by the large volume-expansion of silicon during high discharge and charge conditions [18], [21]; **(c) Solid-State-Electrolyte (SSE)**: which solves safety concerns of traditional liquid electrolytes, also improving mechanical strength, energy density and life-cyle, while showing limited drawbacks, mainly related to costs [22].

For what concerns the second objective, at least three interesting solutions can be identified: **(e) ultra high-power cells**: which are able to achieve very high-power densities starting from standard high-energy chemistries through the optimization of active material and collectors thicknesses, electrolyte composition, and by means of special manufacturing processes, at the price of a significant energy density loss; **(f) Lithium Titanate Oxide (LTO) anodes**: which represent good candidates to overcome the fast charge/discharge rate limitations of traditional carbon anodes [23], [24], which, however, show a significant reduction of energy density to have a stable chemical structure able to tolerate very high rates; **(g) Niobium-based anodes**: which represent an emerging technology aiming at finding a compromise between power and energy densities [25], [26]; in fact Niobium (Nb) tolerates faster rates than standard graphite-based anodes, with a supposed lower reduction of energy density with respect to LTO.

The cell model discussed in Section III-C is parametric so to be representative of the standard cells and also some of the emerging technologies. Regarding the latter, we considered those who have already reached a sufficient level of maturity (also testified by the availability of sufficient data). When dealing with high-power cells, we considered the solution **(e)** proposed by Saft [27], constituted by standard NCA/C chemistry, which reaches high-power density – up to 13.3 kW/kg – thanks to an optimized manufacturing process, paying the price of a significant energy density loss (60 kWh/kg). A compromise can be found in the fast-charging Niobium-based solutions **(g)**, discussed in [25], [26] currently in development by Nyobolt and Toshiba. When dealing with high-energy cells, we included the Lithium-metal anodes prototypes **(a)** discussed in [20] and [28] along with the Silicon-based solutions **(b)** proposed by Amprius [29]. Fig. 2 summarizes the considered cell portfolio on the Ragone plot.

When referring to high-power density energy storage systems, supercapacitors (SCs) are also an interesting solution. As a matter of fact, in several studies on H-BPs, they are used as high-power sources, e.g., [11], [14]–[16]. However, supercapacitors currently have a power density ranging from 3 to 14 kW/kg (see some examples provided in [30], [31]), but a rather low energy density, about 1 to 20 Wh/kg. So, without considering any other feature, as safety, aging or costs, ultra high-power cells **(e)** represent a higher performance solution both for power and energy density. Moreover, it should be pointed out how the realization and management of hybrid battery-packs based on Li-ion cells turns out to be rather simple, thanks to the bounded voltage range of Li-ion cells. Opposite, as SC voltage linearly drops with the state of charge, their use would require an ad-hoc design and control of the electronics, e.g., DC/DC converters, to maintain the voltage output within a meaningful operating range [30].

III. Optimal Sizing: Problem Formulation

In order to investigate the possible advantages of hybrid battery packs, different metrics can be taken into account, from installation costs to the energy consumption in specific driving-cycles [32]. In the racing scenario, the crucial objective is represented by the maximization of the vehicle performance, leading to an optimal battery sizing problem, because of the strong impact of the battery size on mass, power limits and mileage, and consequently on the race time.
Starting from the work presented in [9], we formulated a co-design optimization problem (Co-OP) aiming at minimizing the race time t_{race} on a given circuit:

$$\min_{\mathcal{U}} t_{\text{race}}, \tag{1}$$

where $\mathcal{U}$ is the set of optimization variables, that includes both the sizing variables and the ones related to the hybrid battery pack usage during the race. The first step to formulate the Co-OP is the definition of the link between the optimization variables and the race time, therefore a model for vehicle and battery dynamics is introduced.

A. Vehicle model

Point-mass models are deemed to be suitable for *minimum lap time* problems (see e.g., [1], [2]) where the race-line –

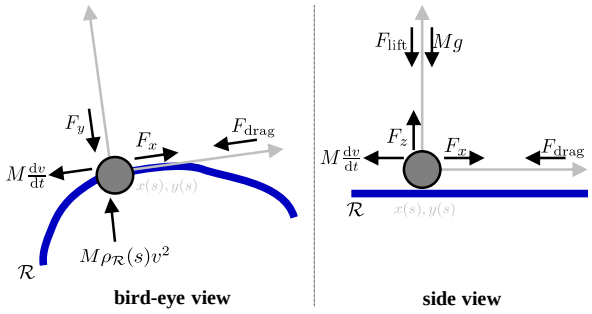

Fig. 3. Bird-eye and side view of the forces acting on the point-mass.

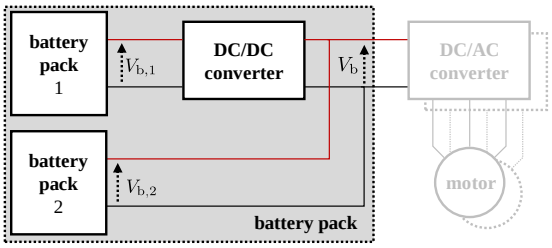

Fig. 4. Schematic representation of the considered hybrid battery pack architecture coupled with the vehicle electric motors, from one to four, depending on the vehicle architecture.

described by planar coordinates x,y and defined along the path abscissa s from 0 to the end of the race s_{race}: $\mathcal{R} = \{(x(s), y(s)), s \in \mathcal{R}_s = [0, s_{\text{race}}]\}$ – is considered known. Indeed, point-mass models represent the main vehicle dynamical features, keeping the complexity of the problem low. This setting is also suited for powertrain sizing approaches within a racing context; as discussed in [9] the adoption of point-mass model yields good levels of approximation even when compared with higher fidelity simulations. More complex models are indeed to be preferred when the focus is set on specific aspects, for instance mechanical design [33], tire wear [34] or independent control of electric motors [35].

Referring to Fig. 3, the developed point-mass model computes the longitudinal dynamics through the force balance:

$$\frac{\text{d}v}{\text{d}t} = \frac{1}{M}\left(F_x - F_{\text{drag}}(v)\right), \tag{2}$$

where v is the speed tangential to the race-line, M is the total mass, sum of the vehicle mass M_{v} and the battery pack one M_{b}. The drag force resistance $F_{\text{drag}} = C_{\text{drag}}v^2$ is proportional to the square of the speed. Finally, F_x is the total longitudinal force provided to the wheels:

$$F_x = \frac{T + T_{\text{br}}}{R_{\text{w}}} \tag{3}$$

where R_{w} is the wheel radius, T_{br} is the braking torque applied by the friction brakes and T is the mechanical torque at the wheel generated by the electric motors, that could be either positive in traction or negative during regenerative braking phases.

Considering that the motion is constrained on the race-line $\mathcal{R}$, lateral dynamics effects appear as a constraint, representative of the frictional ellipse limits [36]:

$$\left(\frac{F_x}{\mu_x}\right)^2 + \left(\frac{F_y}{\mu_y}\right)^2 \leq F_z^2, \tag{4}$$

where μ_x and μ_y are the longitudinal and lateral friction peaks. Lateral and vertical forces can be expressed as:

$$\begin{aligned} F_y &= M\rho_{\mathcal{R}}(s)v^2 \\ F_z &= Mg + F_{\text{lift}} \end{aligned} \tag{5}$$

where F_y counteracts the centrifugal force and $\rho_{\mathcal{R}}(s)$ is the race-line curvature at current path abscissa s and g is the gravity acceleration. Eventually, $F_{\text{lift}} = C_{\text{lift}}v^2$ represents the aerodynamic downforce, itself proportional to the square of the speed.

B. Hybrid battery pack model

Hybrid battery packs of Li-ion cells are composed of two different kinds of batteries in parallel. Thanks to the presence of additional power electronics, it is possible to adapt the different cell voltage levels [10], before being applied to the load, represented by the vehicle motors and the related drivers. There exist different electronic architectures that can be used to set up an H-BP [37], involving single or multiple, mono- or bi-directional, DC/DC converters [10], or multi-port DC/DC converters properly designed for this particular application (e.g., [38], [39]). In this work, we consider the simplest configuration, shown in Fig. 4, that is characterized by the presence of a single ideal DC/DC converter coupled with one of the two batteries. This ideal configuration neglects the losses on the DC/DC and assumes that it is properly controlled in order to split the current in each batteries as desired. It follows that the total battery power P_{b} is the sum of the contributions of each battery pack:

$$P_{\text{b}} = P_{\text{b},1} + P_{\text{b},2} = V_{\text{b},1}I_{\text{b},1} + V_{\text{b},2}I_{\text{b},2}. \tag{6}$$

In (6), $I_{\text{b},i}$ represents the current of the i-th battery pack, that is a control variable, while the voltage $V_{\text{b},i}$ is a function of each battery pack model.

The battery model must be able to properly represent the following two main aspects: 1) the battery energy losses which limit the overall disposable energy; 2) the power limitations imposed by the cell voltage bounds. Therefore, a model for each single battery pack, suitable for these kinds of problems, is a static equivalent circuit (also used in [3], [9]). Indeed, the equivalent internal resistance is the main responsible for the battery internal losses and for the reaching of the voltage limits, due to the voltage drop on the internal resistance itself. It follows that the *i*-th battery voltage $V_{\text{b},i}$ is the open-circuit voltage (ocv) $V_{\text{oc},i}(\text{SoC}_i)$ reduced by the drop on the internal resistance $R_{\text{b},i}$ proportional to the battery current $I_{\text{b},i}$ (positive when delivered):

$$V_{\text{b},i} = V_{\text{oc},i}(\text{SoC}_i) - R_{\text{b},i} \cdot I_{\text{b},i},\ i = 1, 2 \tag{7}$$

where SoC_i is the state of charge of the *i*-th battery. Its rate is defined as the ratio between the delivered current and the capacity $Q_{\text{b},i}$ in As:

$$\frac{\text{dSoC}_i}{\text{d}t} = -\frac{I_{\text{b},i}}{Q_{\text{b},i}},\ i = 1, 2. \tag{8}$$

To take into account the limits of the cells operating region, hard constraints on voltage $(V_{\min,i}, V_{\max,i})$ and current $(I_{\min,i}, I_{\max,i})$ are necessary:

$$\begin{matrix} V_{\min,i} \leq V_{\mathrm{b},i} \leq V_{\max,i} \\ I_{\min,i} \leq I_{\mathrm{b},i} \leq I_{\max,i} \end{matrix} , \; i = 1, 2. \tag{9}$$

Recalling that a battery pack is a composed of a number of cells in parallel $\mathcal{P}$ and in series $\mathcal{S}$, the parameters of the equivalent circuit can be written as functions of the cell's ones. Introducing the i-th cell open-circuit voltage v_{oc}, resistance r and capacity q, it holds that

$$V_{\mathrm{oc},i} = \mathcal{S} \cdot v_{\mathrm{oc},i}(\mathrm{SoC}_i), \; R_{\mathrm{b},i} = \frac{\mathcal{S}}{\mathcal{P}} \cdot r_i, \; Q_{\mathrm{b},i} = \mathcal{P} \cdot q_i. \tag{10}$$

Similar considerations can be made for the operating limits:

$$\begin{matrix} I_{\bullet,i} = \mathcal{P} \cdot i_{\bullet,i} \\ V_{\bullet,i} = \mathcal{S} \cdot v_{\bullet,i} \end{matrix} , \; \bullet = \min, \max. \tag{11}$$

Finally, the battery power P_{b} is delivered at the wheel by the electric motors, modeled as a constant average efficiency η that includes the motor and inverter losses:

$$T \frac{v}{R_{\mathrm{w}}} = P_{\mathrm{b}} \cdot \eta^{\mathrm{sign}(P_{\mathrm{b}})}. \tag{12}$$

Notice that this model collapse to the single battery systems one, as in [9], simply considering $i = 1$.

We remark that the proposed battery model features two simplifications. Firstly, it neglects the thermal dynamics, considering the presence of an ideal cooling system able to keep the temperature under control, neglecting its additional power consumption. This is motivated by the need to get a numerically tractable optimization, and most importantly to the high dependence of the cooling system parameters from specific details that are hard to be available at the considered stage of the design (e.g., the vehicle layout, which impacts on the the effective area of the exchangers and the battery geometry, the ambient temperature, etc). Secondly, the formulated model neglects the cell dynamics behavior and the associated overpotentials, which are usually described by adding RC components into the equivalent circuit battery model. As a matter of fact, these parameters are not always disclosed by battery manufactures, as they are not of immediate impact on the battery choice. The validity of these assumptions is briefly discussed at the end of the case study analysis in Section V.

C. Cell technology model

In order to define a model for the possible cell technologies to be included in the optimization problem, a database of cells has been firstly derived. It is composed of representatives of the multiple technologies discussed in Section II: from commercialized cells to prototypes of the emerging solutions. Each cell is described by its energy density e, its power density, both in discharge p^{d} and recharge p^{r}, and by its internal resistance r. From this database, we selected and reported in Tab. I, the most interesting cells found. Indeed, given a level of energy density, they represent the current highest achievable performance, both in terms of power densities and internal resistance. Elements in Tab. I span a wide range:

TABLE I
CELLS DATABASE
COMPOSED OF COMMERCIAL AND EMERGING TECHNOLOGIES
(HIGHLIGHTED IN GRAY) USED TO DEVELOP THE CELLS MODEL.

catode /anode	e Wh/kg	p^{d} kWh/kg	p^{r} kWh/kg	r mΩ	reference
NCA/C	60.0	13.3	13.3	0.8	Saft VL5U
NCA/C	74.0	6.7	6.7	0.8	Saft VL12V
NCA/C	120.0	4.6	4.6	0.7	Saft VL34P
NMC/Nb	149.5	4.3	2.9	1.5	[25]
NMC/C	192.6	3.8	0.43	9	Sony VTC5A
NMC/C	241.0	2.1	0.45	13	Sony VTC6
NMC/Li	257.0	0.9	0.49	2.8	Kokam SLPB065
NMC/Li	300.0	0.87	0.29	7	[20]
NMC/Li	350.0	1.1	0.34	14	[28]
NMC/Si	362.6	1.8	0.36	12	Amprius [40]
NMC/Si	410.0	1.2	0.40	30	Amprius [40]

from ultra high-power cells (13.3 kWh/kg) with low energy density (60 Wh/kg) to ultra high-energy cells (410 Wh/kg) with lower power density (1.2 kWh/kg). Moreover, they cover different kinds of technologies: from the standard NMC or NCA cathodes with graphite anodes, to high-power NCA/C realized through specific manufacturing processes, niobium or lithium based anodes, and, finally, the most recent silicon-based nanowired anodes solutions.

Given this subset of cells, the first modeling step is the identification of suitable functions to define the best achievable discharge/recharge power densities and internal resistance for a certain energy density. The outcome of the computation is shown in Fig. 5, where clear correlations can be identified: i.e., the power density reduces when the energy density increases and the internal resistance reduces when the power density increases.

After this step, both a common open-circuit voltage v_{oc} and a common capacity value $q = 3$ Ah are defined, for each cell. Indeed, despite that the ocv has a unique shape for every Li-ion cell, they share common properties [41], as the plateau around the nominal voltage, which is more accentuated in LFP-based cathodes than NMC-based ones, and the drop around the voltage limits. Fig. 6 shows the ocv used in this work with 3.6 V as nominal voltage (v_{nom}) and 2.5–4.2 V as voltage limits ($v_{\min}$ and $v_{\max}$, respectively). As a consequence of this assumption, we fixed also the number of cells in series $\mathcal{S}$ of each battery pack in order to limit the maximum voltage of the battery pack $V_{\max} = \mathcal{S}_i \cdot v_{\max}$. Concerning the capacity, the assumption of considering the same capacity for all cells is not restrictive, since it typically represents a design choice and different sizes of the same cell are commonly available on the market.

Thanks to these modeling assumptions, a battery pack can be completely described by its energy density e_i and $M_{\mathrm{b},i}$. Therefore, these two quantities could be chosen as design variables. Indeed, all the other parameters are uniquely defined given e_i and $M_{\mathrm{b},i}$. From the energy density definition, it is possible to compute the i-th cells mass

$$m_i = \frac{v_{\mathrm{nom}} q}{e_i} \tag{13}$$

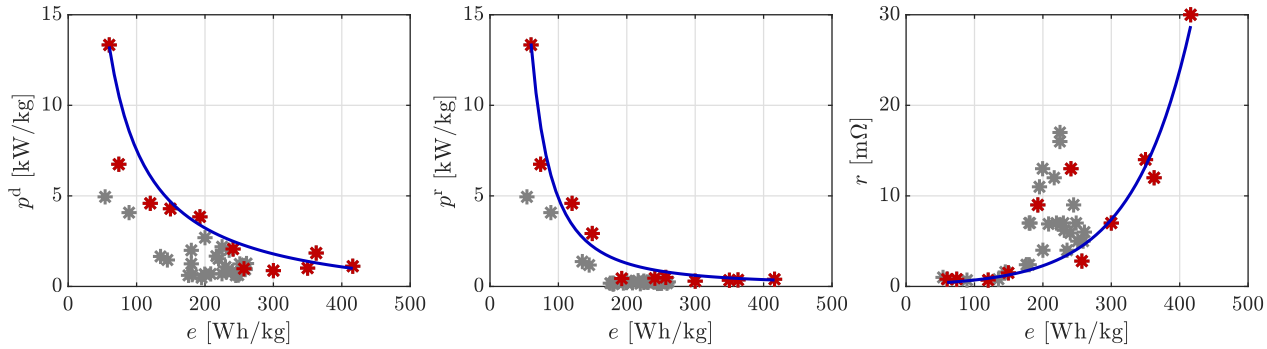

Fig. 5. Correlation fitting results: relations between the cell energy density e and the power density in discharge p^{d} (left) and recharge p^{r} (center), and the internal resistance r (right).

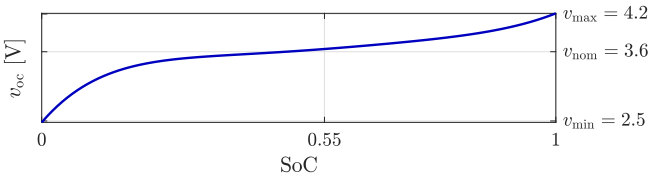

Fig. 6. SoC-dependent open-circuit voltage v_{oc} used in the modeling assumptions.

and the number of cell in parallel in the battery pack:

$$\mathcal{P}_i = \frac{M_{\mathrm{b},i} e_i}{\mathcal{S} v_{\mathrm{nom}} q}. \tag{14}$$

From the power density definition, the current limits can be derived by rearranging (7) in the power domain:

$$i_{\mathrm{max},i} = \frac{v_{\mathrm{nom}} - \sqrt{v_{\mathrm{nom}}^2 - 4 r_i p_i^{\mathrm{d}} m_i}}{2 r_i} \tag{15}$$

and

$$i_{\mathrm{min},i} = \frac{v_{\mathrm{nom}} - \sqrt{v_{\mathrm{nom}}^2 + 4 r_i p_i^{\mathrm{r}} m_i}}{2 r_i}. \tag{16}$$

We highlight that, as a consequence of the assumption of a fixed arbitrary capacity q, the discrete nature of the number of parallels $\mathcal{P}_i$ has been neglected. On the other hand, it must be considered when dealing with a finite set of commercial candidate cells, as in [9].

Finally, another important quantity to be modeled is the battery pack mass M_{b}, that affects the total mass, which already appeared in the vehicle model, in (2) and (5). To account for the additional packaging weight, we introduced a scaling factor $\alpha \leq 1$:

$$M_{\mathrm{b}} = \frac{M_{\mathrm{b},1} + M_{\mathrm{b},2}}{\alpha}. \tag{17}$$

To consider the weight of additional power electronics arising in case of hybrid systems (as discussed in Section III-B), it is possible to define a different value of α for single chemistries and hybrid battery packs:

$$\alpha = \begin{cases} \alpha_{\mathrm{s}}, & \text{for single chemistry battery packs} \\ \alpha_{\mathrm{h}}, & \text{for hybrid battery packs} \end{cases} \tag{18}$$

with $\alpha_{\mathrm{s}} > \alpha_{\mathrm{h}}$.

D. Complete optimization problem

Starting from the derived models, the complete co-design optimization problem (Co-OP) can be formulated. In order to write the problem as a standard optimal control problem (OCP), we employed a spatial-reformulation of the dynamical equations, turning the time into a state variable, while considering the covered space along the race-line $\mathcal{R}$ as the independent one. This reformulation – typical in minimum lap time problems (e.g., [1], [3], [9]) – can be obtained from the following steps:

$$v = \frac{\mathrm{d}s}{\mathrm{d}t} \rightarrow \frac{\mathrm{d}\bullet}{\mathrm{d}s} = \frac{1}{v} \cdot \frac{\mathrm{d}\bullet}{\mathrm{d}t}, \bullet = t, v, \mathrm{SoC}_i. \tag{19}$$

It follows that the cost function can be expressed as:

$$t_{\mathrm{race}} = \int_0^{s_{\mathrm{race}}} \frac{1}{v(s)} \mathrm{d}s, \tag{20}$$

which results to be a suitable form for classical OCPs.

The complete Co-OP is summarized in (21). We recall that the set of optimization variables $\mathcal{U}$ is composed of the two battery currents requested during the race, $I_{\mathrm{b},1}(s)$ and $I_{\mathrm{b},2}(s)$, the dissipative braking torque $T_{\mathrm{br}}(s)$, the size of the two battery packs, represented by $M_{\mathrm{b},1}$, $M_{\mathrm{b},2}$, and its configuration, through e_1, e_2. We also remark that the vehicle EMS during the race is not the output of a pre-defined control strategy, but is implicitly defined by the values of the battery currents; for this reasons, there are no explicit control law parametrizations or SoC target values to be defined.

From (21), it is possible to notice the co-design nature of the problem. Indeed, the optimal control low of $I_{\mathrm{b},i}$ and T_{br} is affected by the battery pack design, as shown by the direct influence of $M_{\mathrm{b},i}$ and e_i on the total vehicle mass and the battery limits. In (21), a few additional constraints on the battery sizing variables have been introduced, in order to limit the energy density range and the battery pack weight. Finally, the constraint $e_1 \leq e_2$ is introduced, considering the symmetry of the problem.

The use of the minimum lap time paradigm is a distinguishing feature of the proposed analysis, compared to the available literature on co-design of H-BP. On the one side, it is based on a cost function, the race time, which naturally fits the objective of the analysis, i.e., how much the use H-BP impact on vehicle dynamic performance. Moreover, the

$$
\begin{aligned}
&\min_{\mathcal{U}} \int_0^{s_{\text{race}}} \tfrac{1}{v}\mathrm{d}s \\
&\text{s.t.} \quad \forall s \in \mathcal{R}_s \text{ and } i = 1,2 \\
&\quad \tfrac{\mathrm{d}t}{\mathrm{d}s} = \tfrac{1}{v} \\
&\quad \tfrac{\mathrm{d}v}{\mathrm{d}s} = \tfrac{1}{v}\tfrac{1}{M}\left(F_x - C_{\text{drag}}v^2\right) \\
&\quad M = M_v + \tfrac{M_{\text{b},1}+M_{\text{b},2}}{\alpha} \\
&\quad \tfrac{\mathrm{dSoC}_i}{\mathrm{d}s} = -\tfrac{1}{v}\tfrac{I_{\text{b}}}{Q_{\text{b}}(e_i, M_{\text{b},i})} \\
&\quad T\tfrac{v}{R_{\text{w}}} = P_{\text{b}}\eta^{\text{sign}(P_{\text{b}})} \\
&\quad P_{\text{b}} = V_{\text{b},1}I_{\text{b},1} + V_{\text{b},2}I_{\text{b},2} \\
&\quad F_x = \tfrac{T+T_{\text{br}}}{R_{\text{w}}} \\
&\quad F_y = M\rho_{\mathcal{R}}v^2 \\
&\quad F_z = Mg + C_{\text{lift}}v^2 \\
&\quad \left(\tfrac{F_x}{\mu_x}\right)^2 + \left(\tfrac{F_y}{\mu_y}\right)^2 \leq F_z^2 \\
&\quad V_{\text{b}} = V_{\text{oc}}(\text{SoC}_i) - R_{\text{b}}(e_i, M_{\text{b},i})I_{\text{b},i} \\
&\quad I_{\min,i}(e_i, M_{\text{b},i}) \leq I_{\text{b},i} \leq I_{\max,i}(e_i, M_{\text{b},i}) \\
&\quad V_{\min,i}(e_i, M_{\text{b},i}) \leq V_{\text{b},i} \leq V_{\max,i}(e_i, M_{\text{b},i}) \\
&\quad 0 \leq \text{SoC}_i \leq 1 \\
&\quad T_{\text{br}} \leq 0 \\
&\quad 0 \leq M_{\text{b},1} + M_{\text{b},2} \leq M_{\text{b,max}} \\
&\quad e_{\min,i} \leq e_i \leq e_{\max,i} \\
&\quad e_1 \leq e_2
\end{aligned}
\tag{21}
$$

adoption of a minimum race time is also necessary since it can properly handle the vehicle mission profile, also called driving-cycle. Indeed, in traditional Co-OP scenarios, the driving-cycle is given *a-priori* and reflects the typical or expected vehicle usage. Technically, within the optimal co-design problem, it plays the role of a constraint that must be satisfied, while addressing the desired optimality criteria (efficiency, cost, space, weight, etc.). Opposite, in the racing scenario, we are addressing how the mission profile directly impacts on the ultimate objective, i.e., minimization of the race time; as such, it is not known in advance and cannot be a-priori fixed in the optimization problem, indeed, it becomes the outcome of the optimization itself.

It should be stressed that these two different ways of handling the vehicle mission profile are not interchangeable. In fact, this is due the feasibility of the driving-cycle, which cannot be generically guaranteed, as it depends on the vehicle dynamics properties; a simple example to frame this idea is to consider how the tire friction ellipse limits the maximum vehicle speed in a turn. H-BP literature typically deals with vehicles like buses, mid-size or small cars and the selected mission profiles are standard(ized) ones that fit the typical usage of the these vehicle. These driving-cycles certainly do not push the vehicle dynamics to its boundaries and, in fact, the employed vehicle dynamics models never include tire-road interaction limitations; as a matter of fact, the feasibility of the driving-cycle is always implicitly assumed, which is a reasonable working hypothesis for the considered scenarios. In our racing application, however, such assumption cannot be done: the vehicle dynamics is pushed to its limits, and the vehicle parameters (for instance, the mass and the battery power limits) highly influence it; thus, a pre-defined driving-cycle cannot be assumed.

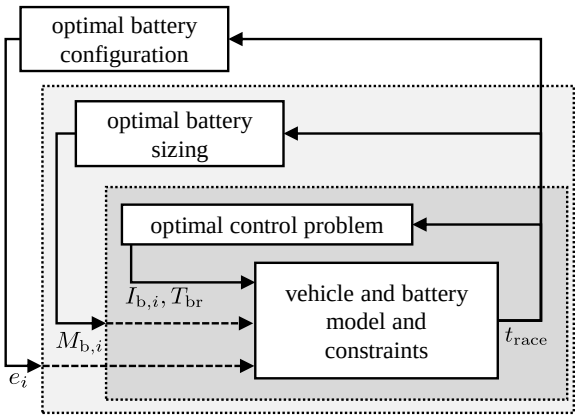

Fig. 7. Multiple-layer optimization scheme.

IV. Optimal Sizing: Numerical Solution

In this section, we discuss how the Co-OP in (21) has been numerically solved. In optimization problems for the sizing of hybrid/electric vehicles powertrains, multiple-layer solutions are often applied [5]. In fact, they simplify the overall numerical solution, breaking it down into simpler subsequent problems, while sharing the same global optimum of the original problem [42]. In this particular context, up to three layers could be defined: an external layer selects the best powertrain configuration, an intermediate one optimizes their size and in internal one computes the time optimal powertrain usage for a particular driving-cycle [5].

For our problem, we extended the methodology discussed in [9] to a triple-layer solution, shown in Fig. 7, where:

- an external layer finds the best configuration of chemistries, using e_1, e_2 as optimization variables;
- an intermediate layer computes the size of the battery pack, optimizing $M_{\text{b},1}$, $M_{\text{b},2}$;
- an internal layer computes the optimal usage of the battery pack, optimizing the current requested to each battery pack $I_{\text{b},1}$, $I_{\text{b},2}$ and the dissipative braking torque T_{br}.

Thanks to the multiple-layer approach, the numerical computation of the solution of (21) becomes easier. Indeed, the **internal layer** becomes a standard nonlinear OCP problem aiming at optimizing the control variables subject to the systems dynamics and fixed constraints. Therefore, the solution can be computed via standard techniques [3], [9], after a suitable time-domain discretization. In our case, we applied the fourth-order explicit Runge-Kutta method [43] with discrete step Δs and the multiple-shooting approach [44] to deal with the problem nonlinearities. Finally, we solved the resulting optimization problem thanks to CasADi [45], using an interior-point based strategy as numerical algorithm.

Once the race time for a particular realization of the battery pack is computed, both the **intermediate** and **external layer** address the solution of a two-dimensional optimization problem. There are different possibilities for the numerical

algorithm to be applied in these layers. Given the nested problem reformulation, each evaluation of the cost function requires the solution of the internal OCP, that is an expensive task in terms of computational load and time. Therefore, to reduce the number of evaluations, we employed the Bayesian Optimization (BO) [46], a gradient-free optimization algorithm well-known for its efficiency (in terms of cost function evaluations).

In conclusion, the main advantage of the layered structure is the simplified search of the solution of the overall problem, by addressing three subsequent optimization problems on a reduced subset of decision variables. Moreover, the proposed three-layered structure requires the solution of two-dimensional problems in the intermediate and external layer; this makes the visualization of the respective cost functions possible, facilitating the analysis of the results, as shown in the case study proposed in Section V.

V. Case Study: Gen3 Formula E

In this case study, we examine the battery sizing for a next Gen3 Formula E cars, whose parameters are listed in Tab. II. The case study focuses on a single circuit, namely the 2021 Rome ePrix shown in Fig. 8. We considered a 23 laps race, corresponding to a distance of 75.9 km, with a discretization interval $\Delta s = 15$ m. To evaluate the full potential of the hybrid battery pack, the power limits given by the current regulations[†] have been neglected.

TABLE II
Vehicle Parameters

vehicle mass	M_{v}	426	kg
wheel radius	R_{w}	34.54	cm
drag coefficient	C_{drag}	0.3927	Ns^2/m^2
aerodynamic coefficient	C_{lift}	0.9526	Ns^2/m^2
friction coefficients	μ_x, μ_y	1.2	-
maximum voltage	$V_{\max}$	878	V
powertrain efficiency	η	0.87	-
packaging factor (single)	α_{s}	0.80	-
packaging factor (hybrid)	α_{h}	0.78	-

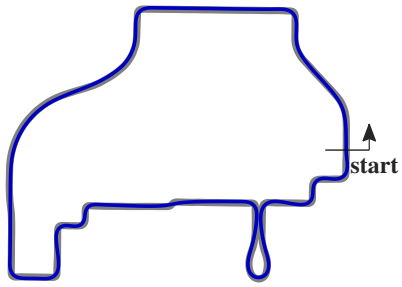

Fig. 8. 2021 Rome ePrix circuit.

As first step, we optimized the single chemistry battery pack. To do so, in the Co-OP (21) $i = 1$ and both the intermediate and external layer become mono-dimensional problems.

[†]FIA Formula E World Championship - Sporting Regulations 2020-2021

A visualization of the optimization results, in particular with respect to the top-level optimization variable, is shown in the left plot of Fig. 9: the achieved minimum race time is 36.7 min and corresponds to an average lap time of 95.74 s; the selected optimal single chemistry has an energy density $e_{\mathrm{b},1} = 181.49$ Wh/kg and a weight $M_{\mathrm{b},1} = 307.96$ kg, generating a total weight of 384.95 kg, including the packaging. Fig. 9 stresses the benefit of optimizing the cell chemistry, considering the convexity of the cost function estimated by the BO.

The most compatible cell of Tab. I with the optimal single battery is the Sony VTC5A. This result can be compared with the one obtained in [9], which also addresses the battery sizing for the Rome ePrix with 23 laps, but for a Formula E Gen2. In that work, the optimization problem returned a higher energy density optimal solution, that is the Sony VTC6 in Tab. I for two main reasons: 1) the Gen2 vehicle is heavier than Gen3, hence it requires more energy; 2) rules were limiting the maximum power (in traction and regeneration) of Gen2 batteries, thus penalizing high power density solutions.

The optimal hybrid battery pack is then computed. The optimization results, again referred to the top-level optimization variables, are shown in the right plot of Fig. 9. The optimal point of the hybrid solution, with 36.25 min of race time (gaining 1.17 seconds per lap), is placed on the boundary of the energy density limits, coupling an ultra high-power battery $e_{\mathrm{b},1} = 60$ Wh/kg and $M_{\mathrm{b},1} = 50$ kg with an ultra high-energy one $e_{\mathrm{b},2} = 410$ Wh/kg and $M_{\mathrm{b},2} = 130$ kg. This solution, named hybrid 60-410, has a total weight of 237.18 kg, resulting in a weight reducing of 147.77 kg compared with the single chemistry one. Referring to Tab. I, this solution implies the use of Saft VL5U cells and the silicon nanowired Amprius ones. Given that the chosen high-energy battery pack is composed of cells that are still prototypes, we also computed the optimal results limiting the region to commercially available cells. In this case, the fastest configuration – named hybrid 60-257 – has a race time of 36.45 min, gaining 0.65 s/lap. Also this configuration combines a high-power battery pack $e_{\mathrm{b},1} = 60$ Wh/kg and $M_{\mathrm{b},1} = 39$ kg with the highest energy one, $e_{\mathrm{b},2} = 257$ Wh/kg and $M_{\mathrm{b},2} = 205$ kg, corresponding to the Kokam SLPB065.

A visual representation on the Ragone plot of the selected

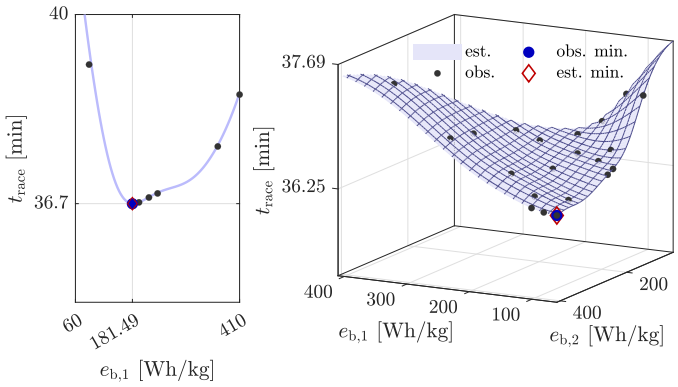

Fig. 9. Optimization results for the single (left) and hybrid (right) battery architectures. In both cases, the observed and the BO estimated cost function are shown, as functions of the top-level decision variables – the cell chemistries.

TABLE III
RESULTS COMPARISON
RACE TIME AND MASS REDUCTION ARE HIGHLIGHTED ALONG WITH HIGH-ENERGY (HEB) AND HIGH-POWER (HPB) BATTERY PACKS CAPACITIES AND ENERGIES.

	single	**hybrid 60-257**	**hybrid 60-410**
race time	36.7 min	36.45 min	36.25 min
gain per lap	-	0.65 s	1.17 s
top speed	272 km/h	277 km/h	277 km/h
total mass	384.95 kg	312.82	237.18
HEB mass	307.96 kg	205 kg	130 kg
HPB mass	-	39 kg	55 kg
package mass	76.99 kg	68.82 kg	52.18 kg
mass reduction	-	72.13 kg	147.77 kg
HEB capacity	55.9 kWh	52.68 kWh	53.3 kWh
HPB capacity	-	2.34 kWh	3.3 kWh
HEB energy discharged	114.91 kWh	69.77 kWh	52.93 kWh
HEB energy recharged	59.73 kWh	17.64 kWh	0.24 kWh
HPB energy discharged	-	49.39 kWh	76.91 kWh
HPB energy recharged	-	46.74 kWh	73.22 kWh
dissipative braking energy	4.59 kWh	0.17 kWh	-

optimal solutions is depicted in Fig. 10 and the numerical details summarized in Tab. III. In general, the hybrid battery pack significantly reduces both the race time and the battery pack weight. These results, despite the simplifying assumptions discussed in the modeling section, show the great potential and impact that H-BPs can have in terms of vehicle dynamics. Considering that the 60-410 solution almost doubles the lap gain performance with respect to the 60-257 configuration, the analysis states also the importance and the benefits that can be expected from the upcoming battery cell technologies. In addition, one should notice that the H-BP Co-OP always selects the values on the boundaries of the available cell portfolio: this supports and motivates research and investments aiming at further improvements in the cell technologies.

The detailed inspection of the time-domain optimization results provides other interesting considerations. In Fig. 11 the outcomes of the internal layer optimization for the different battery packs, in an intermediate lap, are compared. Looking at the speed profile, hybrid based solutions advantages are

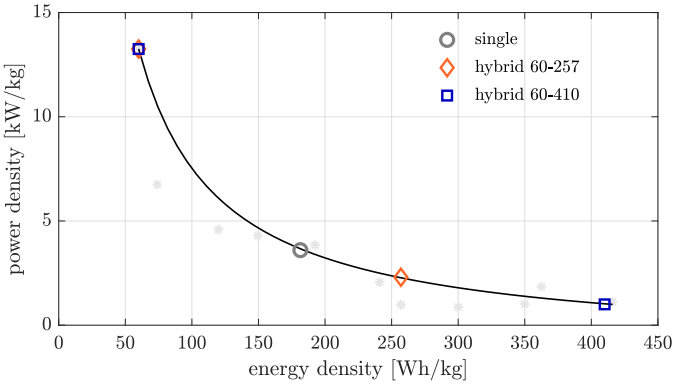

Fig. 10. Visualization the Ragone plot of the optimally selected cell technologies.

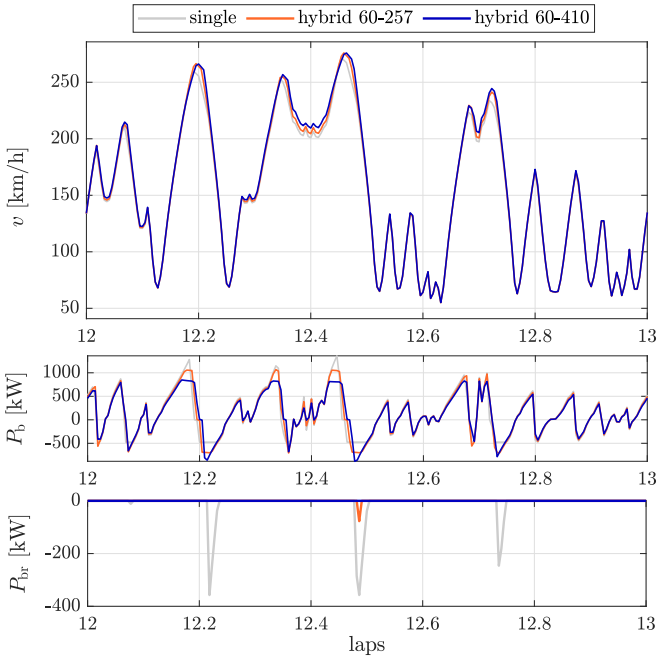

Fig. 11. Comparison between speed profile (top), battery power (middle) and dissipative braking power (bottom) for the optimal single chemistry battery, the 60-257 and 60-410 hybrid configurations.

visible in terms of higher peaks in many parts of the circuit, and later braking points. Analyzing the total battery power demand, despite their higher performance, hybrid solutions are less power demanding, thanks to the weight reduction. This stresses how the battery design parameters highly affect the vehicle mission profiles, remarking the importance of a co-design optimization formulation.

Another interesting aspect to be highlighted is the different use of the brakes: given that the energy dissipated by mechanical brakes is wasted, their use is almost null for the hybrid battery architectures; in these cases the kinetic energy is completely recuperated thanks to the availability of the high-power part of the battery pack.

Focusing on the two hybrid solutions, both hybrid 60-410 and 60-257 share a similar general behavior during the race, see Fig. 12. In fact, the high-energy battery is constantly discharged, while the high-power density SoC oscillates, operating as energy buffer. The evolution of average HPB state of charge is also notable. For most of the race, it is kept close to its maximum value: in this way, the battery voltage is kept high and does not limit the traction performance, which would reduce for lower battery voltage. The HPB is discharged only at the very end of the race, along with the HEB, so to exploit all the available battery energy.

Nonetheless, there are some remarkable differences in the two configurations: to begin with, one can see that the amplitude of the HPB SoC cycle differs in the two cases; in fact, in the 60-410 solution the HEB has a limited power capability, which is compensated by the HPB, explaining its higher SoC fluctuations. Moreover, the battery power split is also very different. In the hybrid 60-257 solution, the HEB actively participates both in traction and regeneration, as quantified in

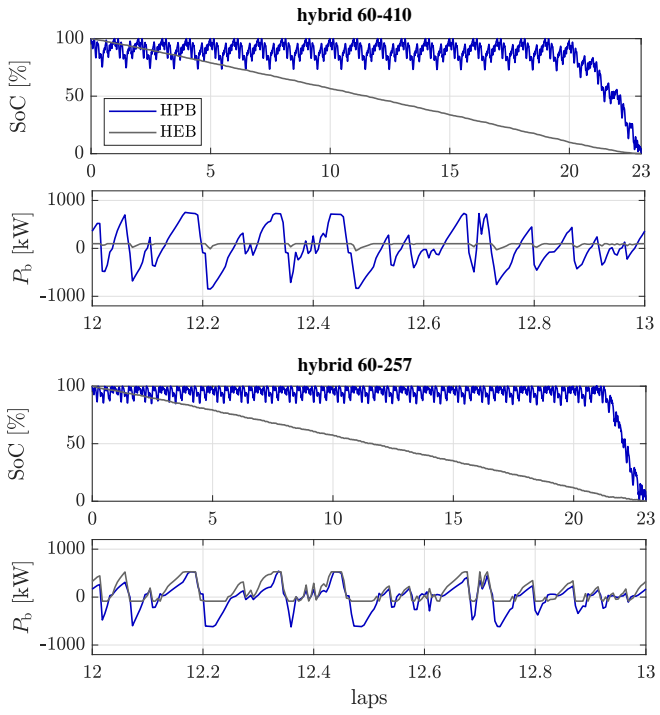

Fig. 12. Comparison of state of charge and power demand for each battery subsystem for the 60-410 and 60-257 hybrid configurations.

Tab. III. In the hybrid 60-410 configuration, opposite, the HEB constantly discharges, even when braking. In fact, in order to maintain the HPB state of charge within its optimal region, it is necessary to recuperate all the energy that the HPB consumes during the traction phase. While, in the 60-257 solution, this energy is low since both HEB and HPB participate in the vehicle acceleration, in the 60-410 one the power limitations of the HEB are so that the HPB is almost entirely responsible for traction. In this last scenario, the energy that can be recuperated is not sufficient to keep the HPB in the desired region of SoC, because of the losses due to the electric motor efficiency and the aerodynamic. This explains why the HEB needs to deliver energy to the HPB in the braking phases as well. Notice that such pattern has already experienced also in traditional vehicles, see [47], [48], whenever the higher energy part of the battery has limited power capabilities.

Despite not being sufficient conditions for optimality, which cannot be easily guaranteed being the optimization problem non-convex, one can say, based on the previous considerations, that resulting optimal solutions are cogent. In addition, also the shape of the external layer estimated cost function in Fig. 9 suggests that there are no other local minima. Hence, the proposed Co-OP, together with quantitative indications on the battery pack composition and its sizing, can be also used to provide interesting guidelines for the development of EMS strategies, specifically tailored for the employed cells and the specific application.

As a concluding remark on the simulation analysis, we recall that among the modeling assumptions there were two aspects that have been neglected. The former is the lack of an active cooling system devoted to the dissipation of the generated thermal power. The second is the absence of the a dynamic model of the battery cells and the related overpotentials. Concerning this last assumption, [11] already revealed that the impact of higher order dynamical models is negligible when computing global optimal sizing solutions, as in our case. Nonetheless, even adopting simplified thermal models, considering the presence of an active cooling system with worst-case scenario parameters and including RC components in the equivalent battery model of the cell, it can be verified that the overall results presented in the paper are not significantly affected. Furthermore, it is important to point out that the optimization is performed in a relative fashion; different designs are compared one against the others. In this way, should a model not be perfectly accurate, we do not expect the relative considerations to vary.

VI. Concluding Remarks

In this work, we analyzed the potential benefits of hybrid battery packs on vehicle dynamics, addressing a minimum lap time co-design problem applied to the Formula E racing scenario. In addition to providing a quantitative indication on the potential of H-BPs on vehicle dynamics, the proposed Co-OP represents a general tool – flexible to variations in vehicle parameters, cell database, competition regulations and number of laps – meant to support the powertrain designer in the choice of cell chemistries, and to provide a quantitative forecast of the battery layout.

The outcome of the co-design optimization problem highlights how the combination of a high-power cell technology, handling traction and regenerative braking, with a high-energy one, reducing the overall battery weight, is able to significantly improve the race time, compared to a traditional single chemistry battery pack.

Additionally, the analysis of the time-domain optimal solutions provides guidelines for the development of real-time energy management strategies. Moreover, it discloses the marginal role of the mechanical braking system providing useful guidelines for its aware design. Eventually it provides an outlook of the potential benefits of emerging and upcoming battery cell technologies.

References

[1] S. Ebbesen, M. Salazar, P. Elbert, C. Bussi, and C. H. Onder, "Time-optimal Control Strategies for a Hybrid Electric Race Car," *IEEE Transactions on Control Systems Technology*, vol. 26, no. 1, pp. 233–247, 2018.

[2] M. Salazar, P. Duhr, C. Balerna, L. Arzilli, and C. H. Onder, "Minimum Lap Time Control of Hybrid Electric Race Cars in Qualifying Scenarios," *IEEE Transactions on Vehicular Technology*, vol. 68, no. 8, pp. 7296–7308, 2019.

[3] T. Herrmann, F. Sauerbeck, M. Bayerlein, J. Betz, and M. Lienkamp, "Optimization-based real-time-capable energy strategy for autonomous electric race cars," *SAE International Journal of Connected and Automated Vehicles*, vol. 5, no. 1, pp. 45–59, 2022.

[4] J. van Kampen, T. Herrmann, and M. Salazar, "Maximum-distance race strategies for a fully electric endurance race car," *European Journal of Control*, p. 100679, 2022.

[5] E. Silvas, T. Hofman, N. Murgovski, L. F. P. Etman, and M. Steinbuch, "Review of optimization strategies for system-level design in hybrid electric vehicles," *IEEE Transactions on Vehicular Technology*, vol. 66, no. 1, pp. 57–70, 2017.

[6] X. Hu, S. J. Moura, N. Murgovski, B. Egardt, and D. Cao, "Integrated optimization of battery sizing, charging, and power management in plug-in hybrid electric vehicles," *IEEE Transactions on Control Systems Technology*, vol. 24, no. 3, pp. 1036–1043, 2016.

[7] O. Sundstrom, L. Guzzella, and P. Soltic, "Torque-assist hybrid electric powertrain sizing: From optimal control towards a sizing law," *IEEE Transactions on Control Systems Technology*, vol. 18, no. 4, pp. 837–849, 2010.

[8] O. Borsboom, C. A. Fahdzyana, T. Hofman, and M. Salazar, "A convex optimization framework for minimum lap time design and control of electric race cars," *IEEE Transactions on Vehicular Technology*, vol. 70, no. 9, pp. 8478–8489, 2021.

[9] G. Riva, S. Radrizzani, G. Panzani, M. Corno, and S. M. Savaresi, "An optimal battery sizing co-design approach for electric racing cars," *IEEE Control Systems Letters*, vol. 6, pp. 3074–3079, 2022.

[10] J. Becker, T. Nemeth, R. Wegmann, and D. U. Sauer, "Dimensioning and Optimization of Hybrid Li-Ion Battery Systems for EVs," *World Electric Vehicle Journal*, vol. 9, no. 2, p. 19, 2018.

[11] C. Pinto, J. V. Barreras, R. de Castro, R. E. Araújo, and E. Schaltz, "Study on the combined influence of battery models and sizing strategy for hybrid and battery-based electric vehicles," *Energy*, vol. 137, pp. 272–284, 2017.

[12] R. E. Araujo, R. de Castro, C. Pinto, P. Melo, and D. Freitas, "Combined sizing and energy management in evs with batteries and supercapacitors," *IEEE Transactions on Vehicular Technology*, vol. 63, no. 7, pp. 3062–3076, 2015.

[13] A. Ostadi and M. Kazerani, "A comparative analysis of optimal sizing of battery-only, ultracapacitor-only, and battery–ultracapacitor hybrid energy storage systems for a city bus," *IEEE Transactions on Vehicular Technology*, vol. 64, no. 10, pp. 4449–4460, 2015.

[14] H. Yu, F. Castelli-Dezza, F. Cheli, X. Tang, X. Hu, and X. Lin, "Dimensioning and Power Management of Hybrid Energy Storage Systems for Electric Vehicles With Multiple Optimization Criteria," *IEEE Transactions on Power Electronics*, vol. 36, no. 5, pp. 5545–5556, 2021.

[15] H. H. Eldeeb, A. T. Elsayed, C. R. Lashway, and O. Mohammed, "Hybrid energy storage sizing and power splitting optimization for plug-in electric vehicles," *IEEE Transactions on Industry Applications*, vol. 55, no. 3, pp. 2252–2262, 2019.

[16] L. Zhang, X. Hu, Z. Wang, F. Sun, J. Deng, and D. G. Dorrell, "Multiobjective optimal sizing of hybrid energy storage system for electric vehicles," *IEEE Transactions on Vehicular Technology*, vol. 67, no. 2, pp. 1027–1035, 2018.

[17] J. Shen, S. Dusmez, and A. Khaligh, "Optimization of sizing and battery cycle life in battery/ultracapacitor hybrid energy storage systems for electric vehicle applications," *IEEE Transactions on Industrial Informatics*, vol. 10, no. 4, pp. 2112–2121, 2014.

[18] Y. Ding, Z. P. Cano, A. Yu, J. Lu, and Z. Chen, "Automotive li-ion batteries: Current status and future perspectives," *Electrochemical Energy Reviews*, vol. 2, no. 1, pp. 1–28, 2019.

[19] S.-T. Myung, F. Maglia, K.-J. Park, C. S. Yoon, P. Lamp, S.-J. Kim, and Y.-K. Sun, "Nickel-rich layered cathode materials for automotive lithium-ion batteries: Achievements and perspectives," *ACS Energy Letters*, vol. 2, no. 1, pp. 196–223, 2017.

[20] C. Niu, H. Lee, S. Chen, Q. Li, J. Du, W. Xu, J.-G. Zhang, M. S. Whittingham, J. Xiao, and J. Liu, "High-energy lithium metal pouch cells with limited anode swelling and long stable cycles," *Nature Energy*, vol. 4, pp. 551–559, 2019.

[21] L. Sun, Y. Liu, R. Shao, J. Wu, R. Jiang, and Z. Jin, "Recent progress and future perspective on practical silicon anode-based lithium ion batteries," *Energy Storage Materials*, vol. 46, pp. 482–502, 2022.

[22] C. Li, Z.-y. Wang, Z.-j. He, Y.-j. Li, J. Mao, K.-h. Dai, C. Yan, and J.-c. Zheng, "An advance review of solid-state battery: Challenges, progress and prospects," *Sustainable Materials and Technologies*, vol. 29, no. e00297, 2021.

[23] H.-G. Jung, M. W. Jang, J. Hassoun, Y.-K. Sun, and B. Scrosati, "A high-rate long-life Li4Ti5O12/Li[Ni0.45Co0.1Mn1.45]O4 lithium-ion battery," *Nature Communications*, vol. 2, no. 1, p. 516, 2011.

[24] B. Gangaja, S. Nair, and D. Santhanagopalan, "Surface-Engineered Li4Ti5O12 Nanostructures for High-Power Li-Ion Batteries," *Nano-Micro Letters*, vol. 12, pp. 1–11, 2020.

[25] N. Takami, K. Ise, Y. Harada, T. Iwasaki, T. Kishi, and K. Hoshina, "High-energy, fast-charging, long-life lithium-ion batteries using TiNb2O7 anodes for automotive applications," *Journal of Power Sources*, vol. 396, pp. 429–436, 2018.

[26] K. J. Griffith, Y. Harada, S. Egusa, R. M. Ribas, R. S. Monteiro, R. B. Von Dreele, A. K. Cheetham, R. J. Cava, C. P. Grey, and J. B. Goodenough, "Titanium niobium oxide: From discovery to application in fast-charging lithium-ion batteries," *Chemistry of Materials*, vol. 33, pp. 4–18, 2020.

[27] K. Nechev, S. Ferguson, T. Guseynov, S. Gargies, and J. Erbacher, "Next Generation Li-Ion Technology from SAFT," *SAE Technical Paper*, pp. 1–6, 2008.

[28] C. Niu, D. Liu, J. A. Lochala, C. S. Anderson, X. Cao, M. E. Gross, W. Xu, J.-G. Zhang, M. S. Whittingham, J. Xiao, and J. Liu, "Balancing interfacial reactions to achieve long cycle life in high-energy lithium metal batteries," *Nature Energy*, vol. 6, pp. 723–732, 2021.

[29] Y. Cui, "Silicon anodes," *Nature Energy*, vol. 6, no. 10, pp. 995–996, 2021.

[30] M. E. Şahin, F. Blaabjerg, and A. Sangwongwanich, "A comprehensive review on supercapacitor applications and developments," *Energies*, vol. 15, no. 3, 2022.

[31] M.-H. Kim, H.-K. Kim, K. Xi, R. V. Kumar, D. S. Jung, K.-B. Kim, and K. C. Roh, "Lithium–sulfur capacitors," *ACS applied materials & interfaces*, vol. 10, no. 7, pp. 6199–6206, 2018.

[32] R. E. Araújo, R. de Castro, C. Pinto, P. Melo, and D. Freitas, "Combined Sizing and Energy Management in EVs With Batteries and Supercapacitors," *IEEE Transactions on Vehicular Technology*, vol. 63, no. 7, pp. 3062–3076, 2014.

[33] H. Yu, F. Cheli, and F. Castelli-Dezza, "Optimal Design and Control of 4-IWD Electric Vehicles Based on a 14-DOF Vehicle Model," *IEEE Transactions on Vehicular Technology*, vol. 67, no. 11, pp. 10 457–10 469, 2018.

[34] W. J. West and D. J. N. Limebeer, "Optimal tyre management for a high-performance race car," *Vehicle System Dynamics*, vol. 60, no. 1, pp. 1–19, 2022.

[35] S. Broere, J. van Kampen, and M. Salazar, "Minimum-lap-time control strategies for all-wheel drive electric race cars via convex optimization," in *2022 European Control Conference (ECC)*, 2022, pp. 1204–1211.

[36] W. Milliken, D. Milliken, and L. Metz, *Race car vehicle dynamics*. SAE International, 1995.

[37] M. J. Lencwe, S. P. D. Chowdhury, and T. O. Olwal, "Hybrid energy storage system topology approaches for use in transport vehicles: A review," *Energy Science & Engineering*, vol. 10, no. 4, pp. 1449–1477, 2022.

[38] Z. Li, O. Onar, A. Khaligh, and E. Schaltz, "Design and control of a multiple input DC/DC converter for battery/ultra-capacitor based electric vehicle power system," in *2009 Twenty-Fourth Annual IEEE Applied Power Electronics Conference and Exposition*, 2009, pp. 591–596.

[39] O. Hegazy, M. El Baghdadi, J. Van Mierlo, P. Lataire, and T. Coosemans, "Analysis and modeling of a bidirectional multiport DC/DC power converter for battery electric vehicle applications," in *2014 16th European Conference on Power Electronics and Applications*, 2014, pp. 1–12.

[40] S. Ionel, "High energy density lithium-ion cells with silicon nanowire anode technology," in *2020 NASA Battery Industry Day*, 2020.

[41] Q.-Q. Yu, R. Xiong, L.-Y. Wang, and C. Lin, "A comparative study on open circuit voltage models for lithium-ion batteries," *Chinese Journal of Mechanical Engineering*, vol. 31, p. 65, 2018.

[42] H. K. Fathy, J. A. Reyer, P. Y. Papalambros, and A. Ulsov, "On the coupling between the plant and controller optimization problems," in *Proceedings of the 2001 American Control Conference*, vol. 3, 2001, pp. 1864–1869.

[43] J. C. Butcher, *The numerical analysis of ordinary differential equations: Runge-Kutta and general linear methods*. Wiley-Interscience, 1987.

[44] M. Kiehl, "Parallel multiple shooting for the solution of initial value problems," *Parallel Computing*, vol. 20, no. 3, pp. 275–295, 1994.

[45] J. A. E. Andersson, J. Gillis, G. Horn, J. B. Rawlings, and M. Diehl, "CasADi: a software framework for nonlinear optimization and optimal control," *Mathematical Programming Computation*, vol. 11, pp. 1–36, 2019.

[46] B. Shahriari, K. Swersky, Z. Wang, R. P. Adams, and N. De Freitas, "Taking the human out of the loop: A review of bayesian optimization," *Proceedings of the IEEE*, vol. 104, no. 1, pp. 148–175, 2015.

[47] C. Kagiri and X. Xia, "Optimal control of a hybrid battery/supercapacitor storage for neighborhood electric vehicles," *Energy Procedia*, vol. 105, pp. 2145–2150, 2017.

[48] C. Capasso, D. Lauria, and O. Veneri, "Optimal control strategy of ultracapacitors in hybrid energy storage system for electric vehicles," *Energy Procedia*, vol. 142, pp. 1914–1919, 2017.

Stefano Radrizzani received B.Sc. and M.Sc. in Automation and Control Engineering from Politecnico di Milano in 2017 and 2019, respectively, discussing a thesis about the braking pressure control of a brake-by-wire actuator for a Formula E. In July 2019, he was selected for a summer camp for elite students by the Hong Kong University of Science and Technology (HKUST). In November 2019, he joined the mOve research group at Politecnico di Milano as a PhD candidate in Systems and Control. His current research is related to energy management, battery sizing and actuators control in vehicles.

Giorgio Riva received his Bachelor's Degree and his Master's Degree cum Laude in Automation Engineering from Politecnico di Milano. He received the Ph.D. cum Laude in Systems and Control Engineering from Politecnico di Milano on November 2021, discussing a thesis about the role of forces in the vehicle dynamics control context. From 2022 he is a Senior Post-Doc researcher inside the mOve research group, resident in Brembo. His main research activities deal with vehicle control and estimation strategies, and optimization.

Giulio Panzani M.Sc in Mechanical Engineering control specialization, 2012) from Politecnico di Milano. He held post-doc positions at the University of Trento and at the Swiss Federal Institute of Technology of Zuerich (ETHZ). He is an Associate Professor with the Dipartimento di Elettronica, Informazione e Bioingegneria, Politecnico di Milano, Italy. His main research interests include the analysis of dynamics, control design, actuation and estimation for two (and four) wheeled vehicles.

Matteo Corno received the Master of Science degree in computer and electrical engineering from the University of Illinois, and the Ph.D. cum laude degree with a thesis on active stability control of two-wheeled vehicles from the Politecnico di Milano, Milano, Italy, in 2005 and 2009. He is an Associate Professor with the Dipartimento di Elettronica, Informazione e Bioingegneria, Politecnico di Milano, Italy. His current research interests include dynamics and control of vehicles (especially electric-hybrid vehicles), Lithium-ion battery modeling, estimation and control.

Sergio M. Savaresi received the M.Sc. in Electrical Engineering (Politecnico di Milano, 1992), the Ph.D. in Systems and Control Engineering (Politecnico di Milano, 1996), and the M.Sc. in Applied Mathematics (Catholic University, Brescia, 2000). After the Ph.D. he worked as management consultant at McKinsey&Co, Milan Office. He is Full Professor in Automatic Control at Politecnico di Milano since 2006 . He is Deputy Director and Chair of the Systems&Control Section of Department of Electronics, Computer Sciences and Bioengineering (DEIB), Politecnico di Milano. He is author of more than 500 scientific publications. His main interests are in the areas of vehicles control, automotive systems, data analysis and system identification, non-linear control theory, and control applications, with special focus on smart mobility. He has been manager and technical leader of more than 400 research projects in cooperation with private companies. He is co-founder of 9 high-tech startup companies.